Cross-polarization coupling of whispering-gallery modes due to the spin-orbit interaction of light

A. T. Rosenberger

A. T. Rosenberger, "Cross-polarization coupling of whispering-gallery modes due to the spin-orbit interaction of light," Proc. SPIE 10904, Laser Resonators, Microresonators, and Beam Control XXI, 109041C (4 March 2019); doi: 10.1117/12.2508013

SPIE.

Event: SPIE LASE, 2019, San Francisco, California, United States

Cross-polarization coupling of whispering-gallery modes due to the spin-orbit interaction of light

A. T. Rosenberger*
Department of Physics, Oklahoma State University, Stillwater, OK, USA 74078-3072

ABSTRACT

Light can couple between TE and TM whispering-gallery modes (WGMs) of a microresonator; the effect is easily observable when those modes are frequency-degenerate, and can result in coupled-mode induced transparency (CMIT). Fitting experimental observations of CMIT with a numerical model in which the cross-polarization coupling strength is a free parameter shows that the coupling strength is typically 10^{-8} – 10^{-7} per round trip. It is shown here that polarization rotation of this magnitude can result from optical spin-orbit interaction through the asymmetry of a WGM. Using the eikonal approximation to describe a WGM, along with asymmetry of the microresonator about its equator, the maximum possible polarization rotation per round trip can be calculated. Then accounting for spatial overlap and phase mismatch of the coresonant WGMs, using coupled-mode theory, gives coupling strengths in agreement with experiment.

Keywords: microresonator, whispering-gallery modes, cross-polarization coupling, optical spin-orbit interaction

1. INTRODUCTION

Two families of orthogonally polarized whispering-gallery modes (WGMs) exist within a dielectric microresonator. These are the transverse electric (TE) and transverse magnetic (TM) modes, which are, ideally, independent of each other. However, it is possible for light to couple between TE and TM modes in a non-ideal resonator. This cross-polarization coupling (CPC) produces observable effects if the two modes are frequency-degenerate (coresonant). The observation[1,2] of coupled-mode induced transparency or attenuation (CMIT, CMIA) or Autler-Townes splitting (ATS) confirms that CPC is an intracavity process. If linearly polarized light is incident on the resonator and the throughput is polarization-analyzed, WGMs of the incident polarization will appear as dips in the throughput power and those of the orthogonal polarization will appear as peaks because of excitation by CPC. Similar effects of polarization conversion can be observed without intracavity coupling,[3-6] but effects like CMIT require it, and we will use the term CPC to imply intracavity coupling. In this paper it will be shown that polarization rotation in a slightly asymmetric microresonator leads to CPC with a strength that agrees with experimental model-fit results.[2] This effect is one manifestation of spin-orbit interaction of the light in a WGM.

Polarization rotation of guided waves due to asymmetries such as tilted sidewalls has long been known and studied.[7-9] It has been observed not only in waveguides but also in resonators.[10-13] Previous work has shown that such asymmetry-based polarization rotation is a result of optical spin-orbit interaction, or a Berry phase effect.[14-16] In these studies and the current work, these are geometrical effects; similar rotation of polarization can also be observed in structures made of birefringent material.[17,18]

Here, it is shown that slight axial asymmetry of a WGM microresonator about its equator leads to CPC through polarization rotation in total internal reflection.[19,20] The interaction of spin and extrinsic orbital angular momentum[21] of light in a WGM results in a reflection phase shift that is different for the two circular polarizations, producing polarization rotation and thus CPC. The WGM is treated in the eikonal approximation,[22,23] making one total reflection per wavelength propagation distance, and the mode asymmetry produces a slight polarization rotation with each reflection. Coupled-mode theory is then used to take into account the phase mismatch between the two orthogonally polarized WGMs and their spatial overlap. This is done for a representative pair of orthogonally polarized coresonant WGMs to get a quantitative estimate of the CPC strength (probability of polarization change per round trip) that compares well with experimental observation.[2]

*atr@okstate.edu; phone 1 405 744-6742; fax 1 405 744-6811; physics.okstate.edu/rosenber/index.html

Laser Resonators, Microresonators, and Beam Control XXI, edited by Alexis V. Kudryashov, Alan H. Paxton, Vladimir S. Ilchenko, Proc. of SPIE Vol. 10904, 109041C · © 2019 SPIE
CCC code: 0277-786X/19/$18 · doi: 10.1117/12.2508013

2. ANALYSIS

Light in a WGM circulates in the equatorial plane of the microresonator, confined by total internal reflection. Because the dimensions of the resonator are orders of magnitude larger than the wavelength of the light, a quasi-classical method, based on the eikonal approximation, gives a very good approximation to the exact WGM eigenfrequencies of the resonator.[22,23] Using this method, a mode is seen as being composed of rays that make m reflections per round trip, with the distance between reflections being one wavelength λ. As seen below, m is one of the three indices that specify a WGM, namely the number of wavelengths around the resonator's circumference. From this, it is easy to see that the angle of incidence of a ray is given by

$$\theta = \frac{\pi}{2} - \frac{\pi}{m}. \tag{1}$$

Now let the orbital angular momentum of the WGM light circulating along the equator be in the z direction, along the resonator axis. After one reflection, the incident TE (s-polarized) field will be accompanied by a TM (p-polarized) component, or vice versa, according to

$$E_{TM} = t_s' E_{TE} \quad \text{or} \quad E_{TE} = -t_p' E_{TM}, \tag{2}$$

where[19,20]

$$t_{s,p}' = \frac{2\langle \beta_z \rangle \cot\theta}{\beta_{TE,TM}}. \tag{3}$$

Here $\beta_{TE,TM}$ is the propagation constant of the light in the incident WGM; for polarization rotation to occur, clearly its average axial component $\langle \beta_z \rangle$ must be nonzero, thus requiring asymmetry of the WGM about the equatorial plane. The rotation probability amplitude (per reflection) t_s' will be many orders of magnitude smaller than unity, so higher-order corrections from Ref. 19, including a complex term with phase equal to the very small s-p reflection phase difference, have been neglected.

In order to make a quantitative estimate of the CPC strength, the microresonator and its WGMs need to be specified. We have used microspheres and hollow bottle resonators[24-27] for studying CMIT.[2] Because of its various advantages such as usage for internal sensing and ease of strain tuning, the hollow bottle resonator (HBR) is more convenient and will be considered here. A typical HBR is shown below in Fig. 1.

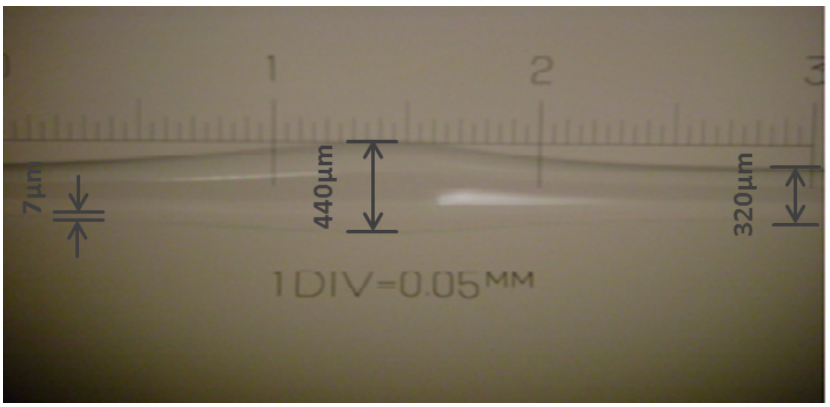

Fig. 1. Hollow bottle resonator (HBR). A fused-silica capillary is etched with HF solution to thin its walls, then heated and pressurized to create the bottle-shaped bulge. The z direction is along the axis of the capillary and resonator, and the equatorial plane is where the diameter is maximum. Note the slight asymmetry about the equatorial plane, resulting from unavoidable non-uniformity in heating while pressurizing.

The bulge in Fig. 1 is somewhat exaggerated; the HBRs that are typically used are made from capillaries of radius 160 µm, with a maximum bulge radius of a = 175 µm, and a wall thickness assumed to be 10 µm for purposes of mode calculations. A WGM in the HBR is characterized by three indices: m, as noted above, is the number of wavelengths in the equatorial circumference; p is the radial order, the number of radial intensity lobes; and q is the axial order, the

number of nodes in the axial field profile. Because of the gentle axial curvature of the bulge, the wave equation approximately separates in cylindrical coordinates, and the amplitude of a WGM (electric field, scalar approximation) is given by

$$E_{mpq}(r,\varphi,z) = E_{TE,TM} R_{mp}(r) Z_{mq}(z) \exp(im\varphi). \tag{4}$$

In Eq. (4), the radial function takes on different Bessel function forms in the three regions. Let b = 165 μm be the inner radius of the HBR, and with A_{mp} representing a normalization constant, we have

$$R_{mp}(r) = \begin{cases} A_{mp}\left[J_m(n_2\beta_0 b) + c_{mp}Y_m(n_2\beta_0 b)\right]\dfrac{J_m(n_1\beta_0 r)}{J_m(n_1\beta_0 b)}, & r < b \\ A_{mp}\left[J_m(n_2\beta_0 r) + c_{mp}Y_m(n_2\beta_0 r)\right], & b < r < a \\ A_{mp}\left[J_m(n_2\beta_0 a) + c_{mp}Y_m(n_2\beta_0 a)\right]\dfrac{H_m^{(1)}(n_3\beta_0 r)}{H_m^{(1)}(n_3\beta_0 a)}, & a < r \end{cases}, \tag{5}$$

where β_0 is the vacuum propagation constant and n_1, n_2, and n_3 are the refractive indices in the three regions – interior, within the silica wall, and exterior, respectively. Given β_0 (within a narrow range), multiple solutions will exist for various combinations of m and p, having p radial lobes of intensity and mixing parameters c_{mp}. Let $\rho(z)$ be the outer radius of the resonator at axial position z, where z = 0 at the equator and $\rho(0) = a$. The shape of the bulge near the equator can be approximated as

$$\rho(z) = \rho(0)\left[1 + (\Delta k z)^2\right]^{-1/2}, \tag{6}$$

where Δk is an inverse length characterizing the change in radius with z. The harmonic oscillator profile of Eq. (6) means that the axial function has the approximate form

$$Z_{mq}\left(\frac{z}{\sigma_z}\right) = B_q(\sigma_z) H_q\left(\frac{z}{\sigma_z}\right)\exp\left(-\frac{z^2}{2\sigma_z^2}\right), \quad \text{where} \quad \sigma_z = \sqrt{\frac{a}{m\Delta k}}. \tag{7}$$

The axial function is a Gaussian multiplied by a Hermite polynomial and a normalization constant.

If the internal evanescent fraction is very small, the WGM is nearly the same as that of a solid bottle resonator, and its frequency is given approximately by[22,24,25,28]

$$\nu_{mpq} \cong \frac{cm}{2\pi a n_2}\left[1 + \frac{\alpha_p}{(2m^2)^{1/3}} - \frac{Ns}{m(N^2-1)^{1/2}} + \frac{3\alpha_p^2}{10(2m^2)^{2/3}} + \frac{N^3 s\left(\frac{2}{3}s^2 - 1\right)\alpha_p}{(2m^5)^{1/3}(N^2-1)^{3/2}} + \frac{\left(q+\frac{1}{2}\right)\Delta k a}{m}\right] \cong \frac{cm}{2\pi a n_{eff}}. \tag{8}$$

In Eq. (8), α_p is the negative of the p^{th} zero of the Airy function, $N = n_2/n_3$, s = 1 for TE modes and $s = 1/N^2$ for TM modes, and n_{eff} is the effective index of the WGM, so that its propagation constant is $\beta = n_{eff}\beta_0$.

The Fourier transform of the axial function is

$$Z_{mq}\left(\frac{\beta_z}{\sigma_\beta}\right) = B_q(\sigma_\beta) H_q\left(\frac{\beta_z}{\sigma_\beta}\right)\exp\left(-\frac{\beta_z^2}{2\sigma_\beta^2}\right), \quad \text{where} \quad \sigma_\beta = \frac{1}{\sigma_z} = \sqrt{\frac{m\Delta k}{a}}, \tag{9}$$

which will result in a zero $\langle\beta_z\rangle$ if the WGM is symmetric about the equator. However, if the bulge is asymmetric, with slightly different curvature above and below the equator, the axial function can be approximated using Δk_+, σ_{z+}, and $\sigma_{\beta+}$ above the equator and Δk_-, σ_{z-}, and $\sigma_{\beta-}$ below the equator. Then

$$\langle \beta_z \rangle = \int_0^\infty \beta_z Z_{mq}^2 \left(\frac{\beta_z}{\sigma_{\beta+}} \right) d\beta_z - \int_0^\infty \beta_z Z_{mq}^2 \left(\frac{\beta_z}{\sigma_{\beta-}} \right) d\beta_z \tag{10}$$

will be nonzero.

The effect of spatial overlap and phase mismatch can be accounted for by using the methods of coupled-mode theory[29] to write, for the amplitude coupled into the TM mode in one reflection,

$$E_{TM} = t_s' E_{TE} i C_{TETM} \int_0^{2\pi/m} \exp\left(i\Delta\beta a\varphi\right) d\varphi \,, \tag{11}$$

where we have used $m\varphi = \beta a\varphi$ in Eq. (4), $\Delta\beta = \beta_{TE} - \beta_{TM} = \left(n_{effTE} - n_{effTM}\right)\beta_0$, and

$$C_{TETM} = \frac{\beta_{TE}^2 - \beta_{TM}^2}{2\beta_{TM}} \int_0^\infty R_{mp}(r) R_{m'p'}(r) r dr \int_{-\infty}^\infty Z_{mq}\left(\frac{z}{\sigma_z}\right) Z_{m'q'}\left(\frac{z}{\sigma_z'}\right) dz \,, \tag{12}$$

in which the primed indices are for TE and the unprimed are for TM. Then the CPC strength resulting from the m reflections in one round trip is denoted by

$$T_s = \left(m t_s' C_{TETM}\right)^2 \frac{\sin^2\left(\frac{\Delta\beta}{2}\frac{2\pi a}{m}\right)}{\left(\frac{\Delta\beta a}{2}\right)^2} \,. \tag{13}$$

3. COMPARISON WITH EXPERIMENT

In order to compare results of the analysis described in the previous section to experimentally determined values of CPC strength, we need to assume specific parameters of the HBR and of the two coupled WGMs to be used in the calculation. The input light of TE polarization is taken to have a vacuum wavelength of 1550 nm, where the refractive index of fused silica is $n_2 = 1.444$ (it is assumed that $n_1 = n_3 = 1$). At the equator, the outer radius of the HBR is $a = 175$ μm and the inner radius is $b = 165$ μm. Each WGM is characterized by the set (m, p, q, n_{eff}), and we take for TE the set (981, 3, 3, 1.3845) and for TM the set (959, 5, 5, 1.3578). Their radial intensity profiles are shown in Fig. 2.

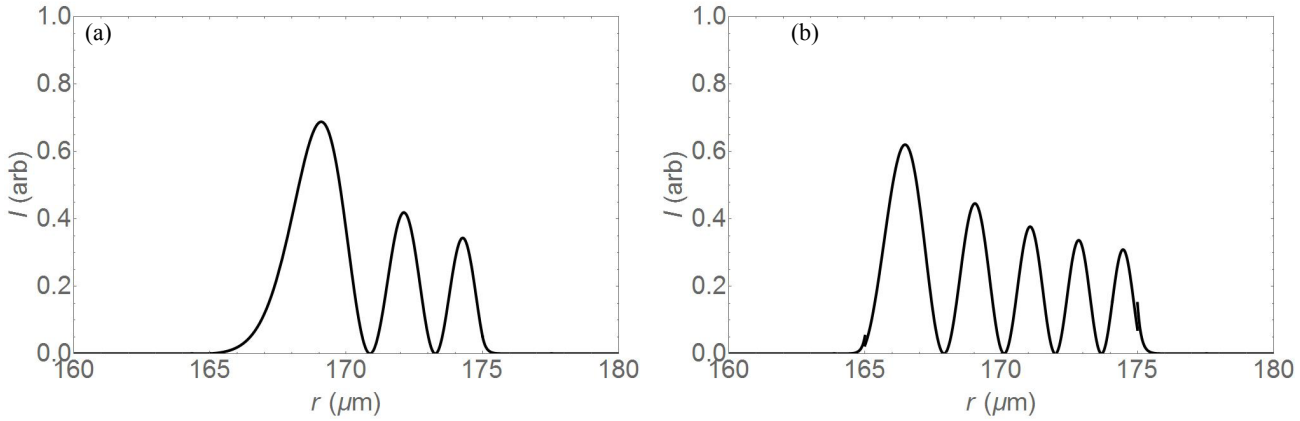

Fig. 2. Radial mode profiles for the two coupled WGMs excited by input light of 1550 nm vacuum wavelength. The outer radius of the HBR is $a = 175$ μm, the inner radius is $b = 165$ μm. (a) TE, $p' = 3$. (b) TM, $p = 5$.

The asymmetry assumed here is characterized by specifying the outer radius of the HBR at z positions 0.5 mm above and below the equator: $\rho(+0.5\text{ mm}) = 171.8$ μm, and $\rho(-0.5\text{ mm}) = 172.4$ μm. These typical values, estimated from measurements made on photographs such as Fig. 1, give a predicted strength for the CPC from this TE mode to this TM mode of $T_s = 2.82\times10^{-7}$. This value is near the upper limit of experimentally determined CPC strengths;[2] observed values range from about that upper limit to three orders of magnitude smaller, with typical values in the 10^{-8} range,[2,30] such as the case shown in Fig. 3.

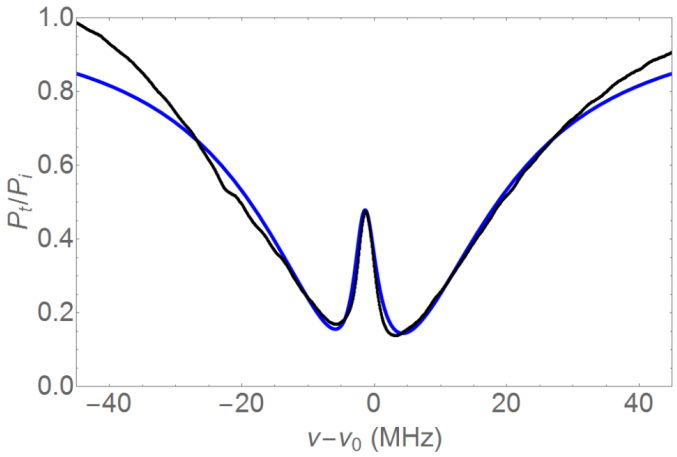

Fig. 3. CMIT with 172-μm-radius HBR.[2] Experimental (black) and steady-state model (blue) throughput spectra. From the fit to the steady-state model, it is found that $T_s = 2.24\times10^{-8}$.

Since the size of the HBR is much larger than a wavelength ($m >> 1$), it is not possible to precisely identify the mode numbers (m, p, q) of the WGMs that are coupled in an experiment such as that of Fig. 3, but the mode numbers are not needed for the steady-state model. Based on the density in frequency of observed WGMs, we estimate that their p values range from 1 to about 10 and their q values from 0 to about 10. Given these ranges, perhaps it is not surprising that the predicted T_s is near the upper observed limit, since the p and q values of the two WGMs used in the calculation are not very different and the resulting C_{TETM} is therefore larger than one found at random would be.

4. CONCLUSIONS

Polarization rotation on total internal reflection is shown to account for the strength of intracavity coupling of WGMs of orthogonal polarizations. With a small axial asymmetry, this is a manifestation of the optical spin-orbit interaction. The predicted CPC strength agrees with that found by two experimental methods using CMIT: steady-state model fit,[2] as in Fig. 3, and input amplitude modulation response.[30] Questions that remain open concern the effect of the mode numbers of the two WGMs and of the HBR wall thickness. If the wall is thinner, higher-order radial modes will have a significant internal evanescent component, affecting their effective refractive indices. Work is underway to derive an expression similar to Eq. (8) that accounts for the inner boundary as well as the outer.

ACKNOWLEDGMENT

Several former and current students have contributed to the experimental and model-fitted values for the CPC strength, to which the results of this work can be compared. They are: Elijah B. Dale, Khoa V. Bui, Erik K. Gonzales, Deepak Ganta, Limu Ke, and Sreekul Raj Rajagopal.

REFERENCES

[1] Rosenberger, A. T., "EIT analogs using orthogonally polarized modes of a single whispering-gallery microresonator," Proc. SPIE 8636, 863602 (2013).

[2] Bui, K. V. and Rosenberger, A. T., "Experimental study of induced transparency or absorption and slow or fast light using orthogonally polarized whispering-gallery modes of a single microresonator," Proc. SPIE 9763, 97630W (2016).

[3] Guan, G. and Vollmer, F., "Polarized transmission spectra of the fiber-microsphere system," Appl. Phys. Lett. 86, 121115 (2005).

[4] Konishi, H., Fujiwara, H., Takeuchi, S., and Sasaki, K., "Polarization-discriminated spectra of a fiber-microsphere system," Appl. Phys. Lett. 89, 121107 (2006).

[5] Bianucci, P., Fietz, C. R., Robertson, J. W., Shvets, G., and Shih, C.-K., "Polarization conversion in a silica microsphere," Opt. Express 15, 7000-7005 (2007).

[6] Bianucci, P., Fietz, C. R., Robertson, J. W., Shvets, G., and Shih, C.-K., "Whispering gallery mode microresonators as polarization converters," Opt. Lett. 32, 2224-2226 (2007).

[7] Peng, S.-T. and Oliner, A. A., "Guidance and Leakage Properties of a Class of Open Dielectric Waveguides: Part I – Mathematical Formulations," IEEE Trans. Microwave Theory Tech. MTT-29, 843-855 (1981).

[8] Oliner, A. A., Peng, S.-T., Hsu, T.-I., and Sanchez, A., "Guidance and Leakage Properties of a Class of Open Dielectric Waveguides: Part II – New Physical Effects," IEEE Trans. Microwave Theory Tech. MTT-29, 855-869 (1981).

[9] Lui, W. W., Hirono, T., Yokoyama, K., and Huang, W.-P., "Polarization Rotation in Semiconductor Bending Waveguides: A Coupled-Mode Theory Formulation," J. Lightwave Technol. 16, 929-936 (1998).

[10] Little, B. E. and Chu, S. T., "Theory of Polarization Rotation and Conversion in Vertically Coupled Microresonators," IEEE Photon. Technol. Lett. 12, 401-403 (2000).

[11] Morichetti, F., Melloni, A., and Martinelli, M., "Effects of Polarization Rotation in Optical Ring-Resonator-Based Devices," J. Lightwave Technol. 24, 573-585 (2006).

[12] Nguyen, T. G., Tummidi, R. S., Koch, T. L., and Mitchell, A., "Lateral leakage in TM-like whispering gallery mode of thin-ridge silicon-on-insulator disk resonators," Opt. Lett. 34, 980-982 (2009).

[13] Bykov, D. A. and Doskolovich, L. L., "Cross-polarization mode coupling and exceptional points in photonic crystal slabs," Phys. Rev. A 97, 013846 (2018).

[14] Schwefel, H. G. L., Stone, A. D., and Tureci, H. E., "Polarization properties and dispersion relations for spiral resonances of a dielectric rod," J. Opt. Soc. Am. B 22, 2295-2307 (2005).

[15] Morinaga, A., Monma, A., Honda, K., and Kitano, M., "Berry's phase for a noncyclic rotation of light in a helically wound optical fiber," Phys. Rev. A 76, 052109 (2007).

[16] Ma, L. B., Li, S. L., Fomin, V. M., Hentschel, M., Götte, J. B., Yin, Y., Jorgensen, M. R., and Schmidt, O. G., "Spin-orbit coupling of light in asymmetric microcavities," Nat. Commun. 7, 10983 (2016).

[17] Weng, W. and Luiten, A. N., "Mode-interactions and polarization conversion in a crystalline microresonator," Opt. Lett. 40, 5431-5434 (2015).

[18] Werner, C. S., Sturman, B., Podivilov, E., Manjeshwar, S. K., Buse, K., and Breunig, I., "Control of mode anticrossings in whispering gallery microresonators," Opt. Express 26, 762-771 (2018).

[19] Mi, C., Chen, S., Zhou, X., Tian, K., Luo, H., and Wen, S., "Observation of tiny polarization rotation rate in total internal reflection via weak measurements," Phot. Research 5, 92-96 (2017).

[20] Hosten, O. and Kwiat, P., "Observation of the Spin Hall Effect of Light via Weak Measurements," Science 319, 787-790 (2008).

[21] Bliokh, K. Y., Rodriguez-Fortuño, F. J., Nori, F., and Zayats, A. V., "Spin-orbit interactions of light," Nature Photon. 9, 796-808 (2015).

[22] Gorodetsky, M. L. and Fomin, A. E., "Geometrical Theory of Whispering-Gallery Modes," IEEE J. Sel. Topics Quantum Electron. 12, 33-39 (2006).

[23] Pluchon, D., Bêche, B., Huby, N., and Gaviot, E., "Theoretical investigations on optical caustics of spherical microresonators: Analytical expressions of caustics and their asymptotic behaviors, computational simulations," Opt. Commun. 285, 2247-2254 (2012).

[24] Sumetsky, M., "Whispering-gallery-bottle microcavities: the three-dimensional etalon," Opt. Lett. 29, 8-10 (2004).

[25] Murugan, G. S., Petrovich, M. N., Jung, Y., Wilkinson, J. S., and Zervas, M. N., "Hollow-bottle optical microresonators," Opt. Express 19, 20773-20784 (2011).

[26] Stoian, R.-I., Bui, K. V., and Rosenberger, A. T., "Silica hollow bottle resonators for use as whispering gallery mode based chemical sensors," J. Opt. 17, 125011 (2015).
[27] Stoian, R.-I., Lavine, B. K., and Rosenberger, A. T., "pH sensing using whispering gallery modes of a silica hollow bottle resonator," Talanta 194, 585-590 (2019).
[28] Hanumegowda, N. M., Stica, C. J., Patel, B. C., White, I., and Fan, X., "Refractometric sensors based on microsphere resonators," Appl. Phys. Lett. 87, 201107 (2005).
[29] Saleh, B. E. A. and Teich, M. C., [Fundamentals of Photonics], John Wiley & Sons, Hoboken, N. J., 315-320 (2007).
[30] Ke, L., Rajagopal, S. R., and Rosenberger, A. T., "Numerical and experimental study of the dynamics of cross polarization coupling in a whispering-gallery microresonator," Proc. SPIE 10904, to be published.